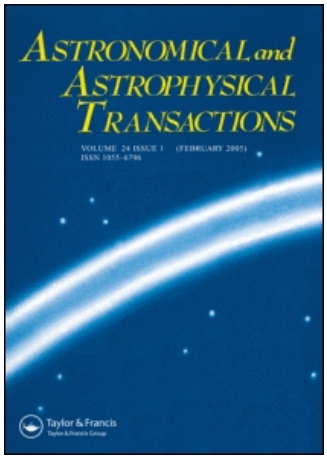

Astronomical & Astrophysical Transactions
The Journal of the Eurasian Astronomical Society
Publication details, including instructions for authors and subscription information:
http://www.informaworld.com/smpp/title~content=t713453505

Restoration of simulated double source images near the resolution limit

V. Yu. Terebizh [a]; O. K. Cherbunina [a]
[a] Sternberg Astronomical Institute, Nauchny, Crimea

Online Publication Date: 01 January 1996
To cite this Article: Terebizh, V. Yu. and Cherbunina, O. K. (1996) 'Restoration of simulated double source images near the resolution limit', Astronomical & Astrophysical Transactions, 9:2, 159 - 170
To link to this article: DOI: 10.1080/10556799608208221
URL: http://dx.doi.org/10.1080/10556799608208221

Astronomical and Astrophysical Transactions, 1995, Vol. 9, pp. 159–170
Reprints available directly from the publisher
Photocopying permitted by license only

RESTORATION OF SIMULATED DOUBLE SOURCE IMAGES NEAR THE RESOLUTION LIMIT

V. Yu. TEREBIZH and O. K. CHERBUNINA

Sternberg Astronomical Institute, 334413 Nauchny, Crimea

(Received November 22, 1993)

The possibility to resolve a double source with point-like components having considerable a priori information has been studied by numerical simulations. The strict form of the Point Spread Function (PSF) was assumed to be known, and the case of equal brightnesses of components was considered. Quite reliable restoration is possible down to separation values smaller by the factor of (Signal-to-Noise)$^{1/2}$ than Rayleigh's boundary. The drop of the estimates accuracy near the theoretical resolution limit has been found to be rather steep.

The use of detector pixels much smaller than the PSF width does not increase essentially the reliability of the object's identification, whereas the use of too coarse image pixels (in the sense of the sampling theorem) strongly reduces the quality of restoration. At the same time, the pixel size in the object space has to be approximately (Signal-to-Noise)$^{1/2}$ times smaller than the PSF width.

KEY WORDS Inverse problems, image restoration

1 INTRODUCTION

The Raylegh's problem (see Rayleigh, 1964, p. 420) of limiting resolution of a double source with the point-like components considered below has been studied many times from various points of view. Early investigations were discussed very clearly by Rautian (1958); among further investigations, those by Schelkunoff (1943), T. di Francia (1955), Wolter (1961), Kozlov (1964), Harris (1964a, b), Frieden (1967), Helstrom (1973), Snyder (see Snyder and Miller, 1991, p. 170), and Lucy (1992a, b) have the most immediate relation to the following considerations.

The aim of the numerical simulations discussed here is to check the expression for theoretical resolution limit in the presence of considerable a priori information presented earlier (Terebizh 1990, 1993), and to study reliability of objects' restoration near the limit.

The following information was supposed to be known a *priori*: 1) the observed blurred and noised image was generated by an object consisting of two incoherent

point-like components of equal brightness; 2) the total brightness of the object F (counts) and the mean intensity of random background (γ_j) (counts/pixel) are known; 3) count fluctuations are subjected to the Poisson distribution; 4) the Point Spread Function (PSF) $h(x-x')$ is exactly known. On the basis of this information and the observed image pattern one has to find the most accurate *estimates* of unknown components' positions and of the distance between them.

Contrary to the approach relating the formulation of the problem to some integral equation, a purely statistical way is considered below, which allows us, in particular, to take into account the *photon noise* (Helstrom, 1969; 1970; Terebizh, 1991). The term "estimate" is considered here in its strict statistical meaning, that is, an estimate of an unknown parameter is some *random variable that depends on the observed pattern*. The first and forth suggestions from those enumerated above are more essential, whereas the others have little effect on the results.

It should be expected on the ground of the above-mentioned investigations that even very close sources with the distance between components smaller than the Rayleigh's limit could be resolved under so considerable a *priori* information. Indeed, it follows from the solution for objects of any shape (Terebizh, 1990; 1993) that with a point source as the only alternative to a double one with point components, the limiting resolution ρ_{min} is equal approximately to

$$\rho_{\min}/\Delta \equiv \mathcal{R} \simeq \left(\frac{z_\alpha + z_\beta}{\psi}\right)^{5/8}, \tag{1}$$

where Δ is some properly defined PSF width, α and β are the error probabilities of the first and the second kind for binary decision rule, z_θ is the Gaussian quantile of the order $|-\theta|$, and ψ is the Signal-to-Noise ratio:

$$\psi = F/(F + 2\Delta\gamma)^{1/2}. \tag{2}$$

We consider here for the sake of simplicity the one-dimensional case with the diffractional PSF:

$$h(x) = \frac{1}{\Delta} \cdot \left[\frac{\sin(\pi x/\Delta)}{\pi x/\Delta}\right]^2; \tag{3}$$

however, equation (1) maintains its validity also for two-dimensional images under corresponding correction of the Signal-to-Noise ratio definition.

Let us take, for example, $F = 10^4$ counts, $\gamma = 10$ counts/pixel, $\Delta = 100$ pixels (the distance from the PSF maximum to the nearest zero), and $\alpha \simeq \beta \simeq 0.10$. Then it follows from (1) and (2) that the Signal-to-Noise ratio is $\psi \simeq 91$, and the limiting relative resolution is $\mathcal{R} \simeq 0.1$. A higher resolving power can be attained when less reliable identification is allowed (say, $\mathcal{R} \simeq 0.05$ for $\alpha \simeq \beta \simeq 1/3$).

The high resolution is conditioned, first of all, by availability of essential a *priori* information. When this information includes only non-negativity of the unknown object and the PSF form, the limiting resolution for double objects with point components is defined by the formula

$$\mathcal{R} \simeq \left(\frac{z_\alpha + z_\beta}{\psi}\right)^{1/4}, \tag{4}$$

which follows from the general solution (Terebizh, 1990). A similar result in the form $\mathcal{R} \propto F^{-1/8}$ was obtained independently by Lucy (1992a, b), who considered the case of zero background (that is $\psi = F^{1/2}$), and used clear approach, based on the image moments, instead of the most powerful test of pattern recognition. The change of the power index from –5/8 to –2/8 when passing from (1) to (4) shows an appreciable deterioration of the limiting resolution (so, $\mathcal{R} \simeq 0.5$ in the conditions of the above-discussed example).

The limits like (1) and (4) can be used both for setting of experiments and for interpretation of observational data, but their real practical significance depends also on a number of indirect circumstances. First of all, it is interesting to ascertain *how steep is the transition to complete indistinguishability of alternative objects.* Just this question in relation to the limit (1) has been studied by Monte Carlo simulations.

2 MODEL OF IMAGE FORMATION

In conformity with the a priori information described above, the model of image formation assumes that the positions (x_1, x_2) of point components of a double object, each of brightness $F/2$, are unknown parameters. The components were blurred randomly and independently from one another, photon by photon, according to the distribution density $h(x)$, and then the random Poisson background of mean intensity $\gamma_j \equiv \gamma$ was added to the stochastically smoothed image. The relation between multinomial statistics under random blurring and Poisson distribution was discussed earlier (Terebizh, 1991), and we shall not return to this item. The brightness distributions are given as sets of integer, non-negative counts at the pixel grid. The pixel sizes in the *object space* and in the *image space* are, in general, different (Snyder, 1990). The resulting probability to obtain some count set $N \equiv (N_1, N_2, \ldots, N_m)$ at the detector pixels is equal to

$$f(N|x_1, x_2) = \prod_{j=1}^{m} \exp(-\lambda_j) \cdot \frac{\lambda_j^{N_j}}{N_j!}, \tag{5}$$

where mean intensity counts are

$$\lambda_j = \frac{F}{2} \cdot [h(j - x_1) + h(j - x_2)] + \gamma_j, \tag{6}$$

and the PSF is defined by (3). Some estimates $\hat{x}_1$ and $\hat{x}_2$ of the parameters x_1 and x_2 are to be found on the basis of the model (5)–(6) and of the observed set of image counts. More exactly, we are now interested not directly in the pair of estimates $(\hat{x}_1, \hat{x}_2)$, but rather in the single estimate of the distance between components as expressed in the units of PSF width:

$$\hat{\theta} \equiv |\hat{x}_1 - \hat{x}_2|/\Delta, \tag{7}$$

true separation of the components $\theta \equiv |x_1 - x_2|/\Delta$ being unknown.

Rather tiny pixellation in the object space should be provided in order to reveal the high-frequency structure of the object (to avoid the so-called *undersampling problem*). Contrary, it is not reasonable to take the image pixels p_i much smaller than the PSF width Δ (see details in Section 4). The particular choice of both scales depends on the observational conditions. Usually one may take $\Delta/2 < p_i < \Delta/3$ for the image pixels, whereas the object pixel size p_0 is determined mainly by the Signal-to-Noise ratio. Indeed, since (1) predicts the size of the restored object's details to be by the factor of the order of $\sqrt{\psi}$ smaller than the PSF width, p_0 should be accepted smaller than Δ at least by the same factor. The main requirement here is to provide the theoretically attainable resolving power in the object space.

The estimates of components' positions are found by means of the Maximum Likelihood (ML) method. This method is known to be unstable with respect of multi-dimensional estimation (Snyder and Miller, 1985; Veklerov and Llacer, 1987; Llacer and Veklerov, 1989; Terebizh and Biryukov, 1993); however, estimates of only two parameters are needed this time, so there are good reasons to use this way now. It means, more exactly, that values $(\hat{x}_1, \hat{x}_2)$ are found by maximization of (5) relative to variables (x_1, x_2), and then the ratio (7) is calculated.

The considered model is more general compared to the model of decisions on binarity discussed in Section 1, where one of only *two* objects types has to be chosen. We should choose one object from *many* alternatives this time (as it is known, the problem of hypothesis testing can be treated as the problem of parameters estimation as well). The present model seems to be more close to the practice, because the true components' separation is almost always unknown to an observer, and he must find its estimate, but not to compare the given object with a single alternative.

3 DISTRIBUTION OF ESTIMATES

The pixel size in the object space was accepted as a linear measure unit in the following consideration ($p_0 = 1$). The Monte Carlo simulations were carried out with two values of the total flux: $F = 10^4$ and 10^6 counts, with the PSF width is $\Delta = 100$ pixels, and the mean background is $\gamma = 10$ counts/pixel. So large width of the PSF has been adopted because of the above-mentioned undersampling problem. The results described in this section have been obtained for pixellation in the image space corresponding to $p_i/\Delta = p_0/\Delta = 1/100$. The check calculations with $p_i/\Delta = p_0/\Delta = 1/200$ do not change our conclusions. The results of calculations with more coarse pixels will be discussed in the next section.

The large number $\mathfrak{N} \sim 10^4$ of random image simulations was performed for every value of true components' separation θ, and each of them was used to calculate the ML- estimates of components' positions and the corresponding separation estimate (7). Since image patterns are random, the estimates $\hat{\theta}$ are different for various patterns. In Figure 1, the sample distribution densities $p(t|\theta)$ of the random variable $\hat{\theta}$ are shown for $F = 10^4$ and a number of true component separation values θ.

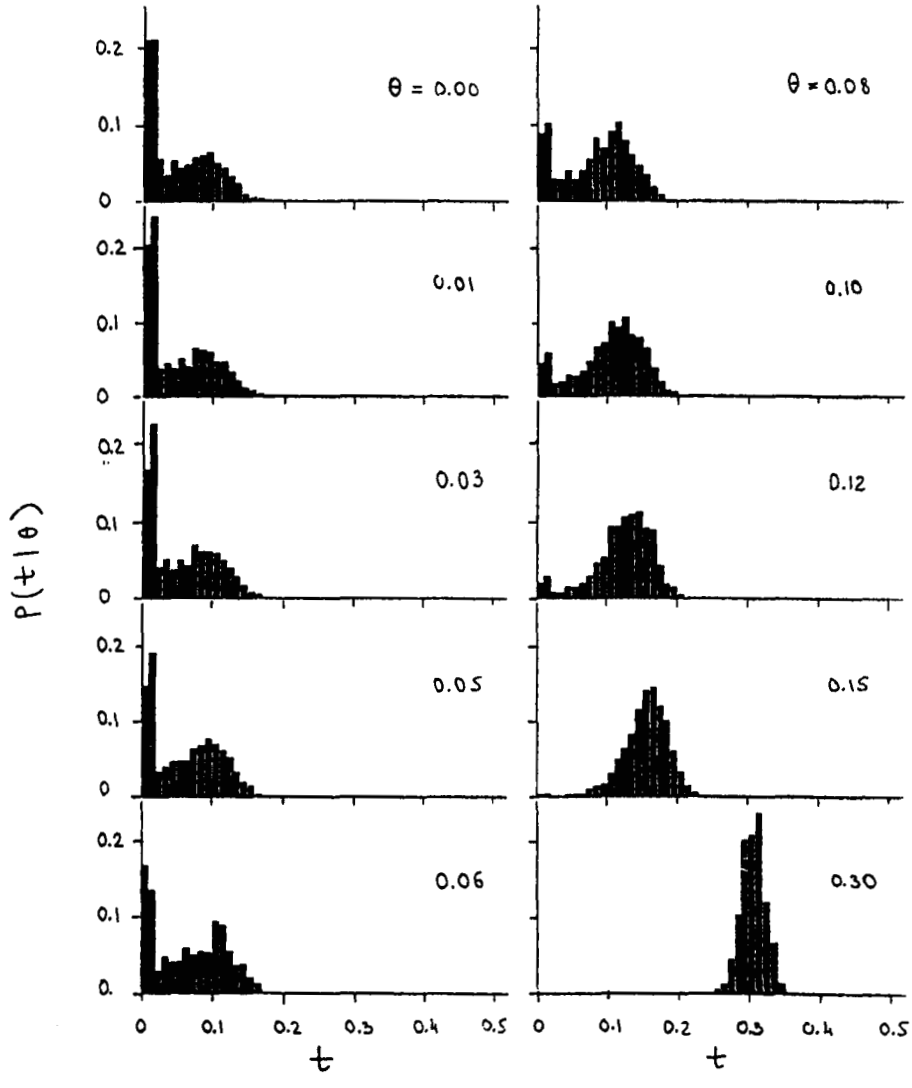

Figure 1 Sample distribution densities of separation estimates $\hat{\theta}$ between components of a double source of total brightness $F = 10^4$ counts for various values of true separation θ.

One can see that the calculated estimates are tightly distributed near the true values when the components are rather far from one another, say, for $\theta = 0.30$ or $\theta = 0.15$. The variance of estimates increases and the single point-like object ($\hat{\theta} = \theta$) is preferred more frequently when the components are drawn together. After reaching some separation value $\theta \simeq 0.06$–0.08, the sample distribution density of estimates does not change practically, so it is completely impossible to recover the parent object on the basis of the observed image. Therefore, the above separation values are to be considered as limiting ones for given conditions. They

Table 1. $(F = 10^4, p_i/\Delta = 0.01)$

θ	$\mathfrak{N}$	$E(\hat{\theta}\|\theta) \cdot 10^2$	$var(\hat{\theta}\|\theta) \cdot 10^4$	$\Omega(\hat{\theta}\|\theta) \cdot 10^4$
0.	45800	4.51±0.02	18.6±0.1	38.9±0.4
0.01	10000	4.50 0.04	18.8 0.3	31.1 0.4
0.03	9800	5.01 0.05	19.8 0.3	23.8 0.3
0.05	10000	5.67 0.05	20.9 0.3	21.3 0.3
0.06	10800	6.26 0.05	23.9 0.3	23.9 0.3
0.08	10000	7.84 0.05	22.8 0.3	22.9 0.3
0.10	23389	9.26 0.03	21.6 0.2	22.1 0.2
0.12	10000	11.63 0.04	17.5 0.3	17.6 0.3
0.15	8550	14.93 0.04	10.8 0.2	10.8 0.2
0.20	25580	20.08 0.02	5.82 0.05	5.83 0.05
0.30	10000	30.10 0.02	2.90 0.04	2.91 0.04

are in satisfactory agreement with the resolution limit (1) for the model of binary decision.

The peak of estimates' distribution for close components observed at $\hat{\theta} = 0$ (that is the primary choice of a single object as an alternative to a double one) can be understood qualitatively if we take into account random image fluctuations. Really, the image patterns with larger width compared to the average one are treated by the algorithm as various double objects, whereas the whole set of patterns more compact than average are treated as a single point-like object. The asymmetrical image fluctuations cause, evidently, only shifts of positional estimates.

It should be noted that some tiny details of sample distributions repeat in more extent calculations, and also after changing the random number generator. Therefore, they cannot be considered as statistical fluctuations. On the other hand, since these details disappear when changing the PSF, they are caused, probably, by particular circumstances of the experiment.

Some numerical data related to the considered case are given in Table 1. Its columns contain: the true components' separation θ; the number of simulations $\mathfrak{N}$; the mean value $\mathbf{E}(\hat{\theta}|\theta)$ and variance $var(\hat{\theta}|\theta)$ of the separation estimates, and also the *scattering* of the estimate:

$$\Omega(\hat{\theta}|\theta) = \mathrm{var}(\hat{\theta}|\theta) + b^2(\hat{\theta}|\theta), \tag{8}$$

where $b(\hat{\theta}|\theta) \equiv \mathbf{E}(\hat{\theta}|\theta) - \theta$ is the estimate's *bias*. The role of the scattering function in the image restoration problem was discussed by Terebizh (1991), where grounds are given also to believe that two-dimensional ML-estimates reach the scattering which is close to the least value attainable theoretically (because of the *information inequality*).

The relation between mean $\mathbf{E}(\hat{\theta}|\theta)$ and true θ values shown in Figure 2 confirms the conclusions inferred from the sample distributions. The mean value of $\hat{\theta}$ not only differs strongly from θ for $\theta < 0.07$, but also poorly depends on it in that range.

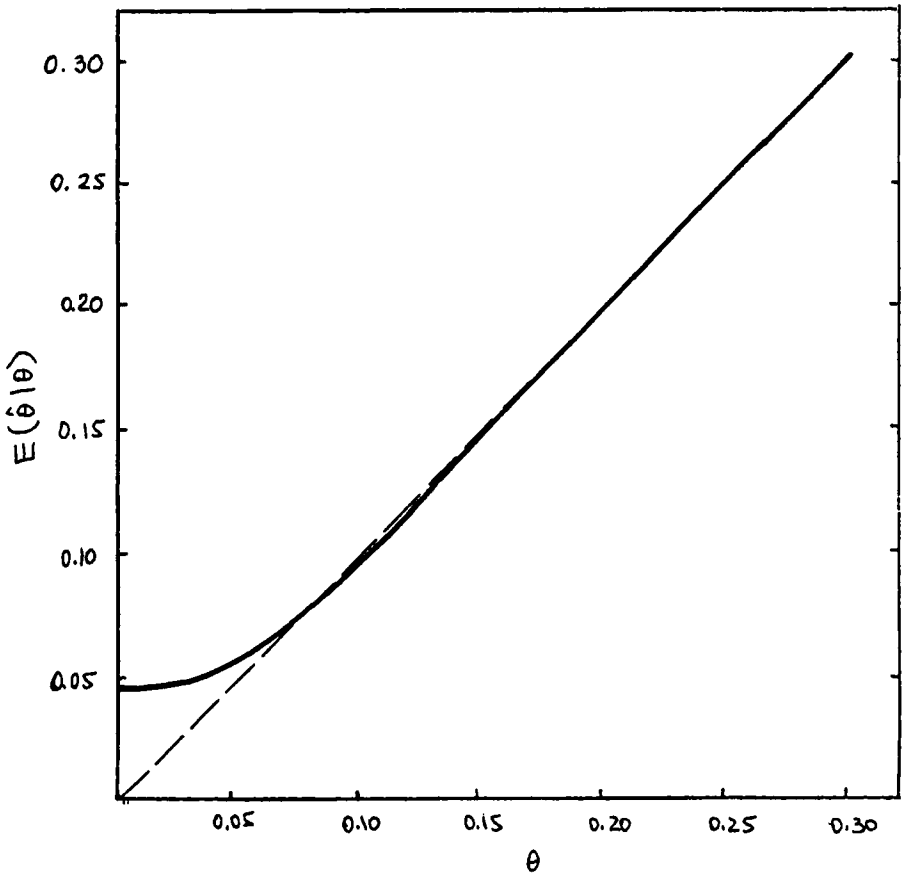

Figure 2 Relation between the mean value of the separation estimates $\mathbf{E}(\hat{\theta}|\theta)$ and the true separation θ for the object's brightness $F = 10^4$ counts.

In order to show the bias of estimates with approaching components and the influence of bias on the scattering value more clearly, we give functions $b(\hat{\theta}|\theta)$ and $\Omega(\hat{\theta}|\theta)$ in Figure 3a, b. It is interesting that the bias is not a monotonous function but changes its sign before deviating from zero. The variance of estimates achieves its maximum value for the critical separation region, and it even decreases for closer separations, like for pulse counters with a non-zero dead time. At last, the relative accuracy of estimates in the region of critical separation values is shown in Figure 3c.

Higher resolving power is expected for brighter objects, of course. Specifically, relation (1) predicts $\mathcal{R} \simeq 0.02$ for $F = 10^6$ counts, and the sample distribution of $\hat{\theta}$ (solid line in Figure 4) is in agreement with this prediction. The corresponding numerical data are given in Table 2. Note that the components are definitely separated when $\theta = 0.10$.

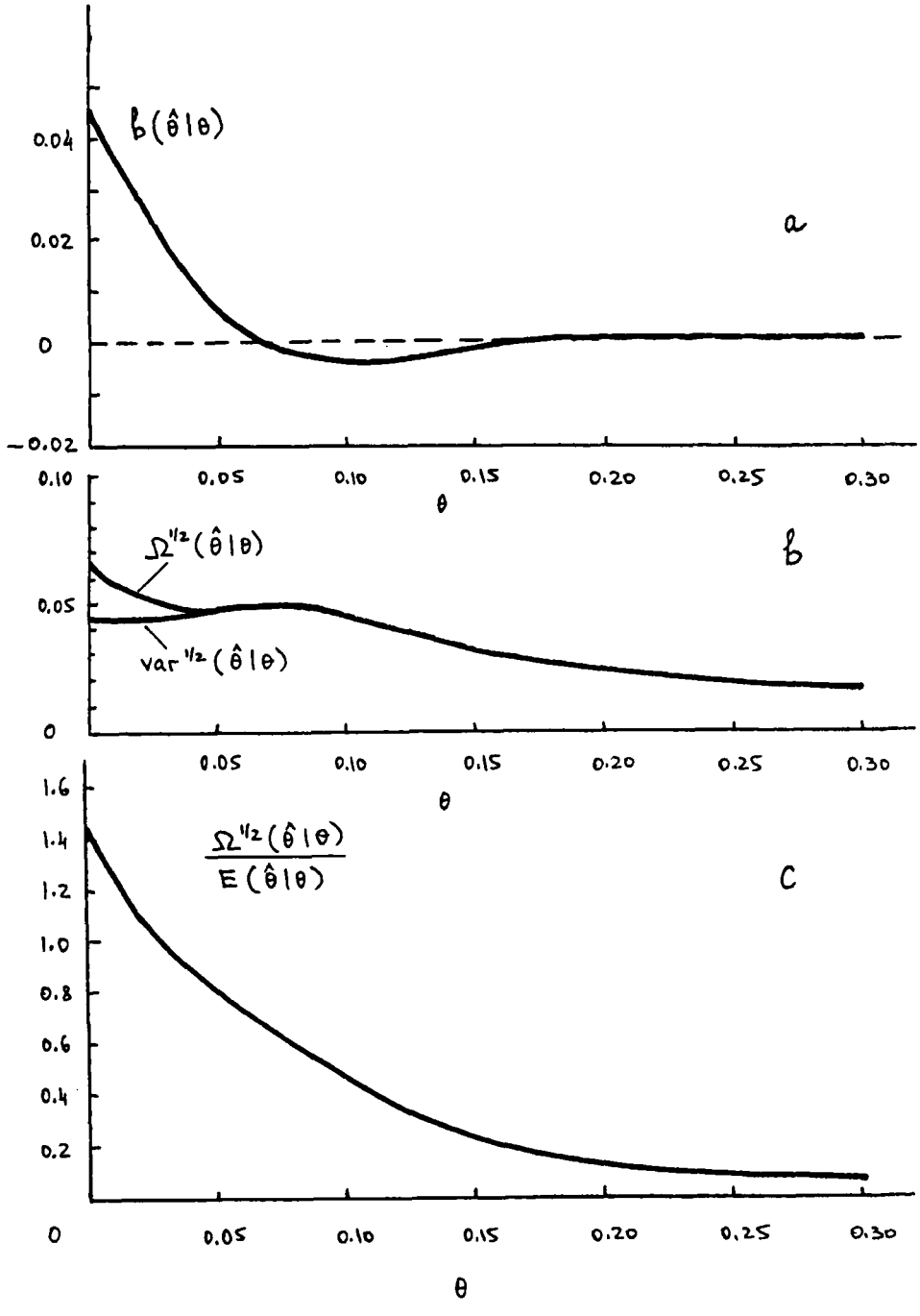

Figure 3 Bias (a), variance and scattering (b), and relative accuracy (c) of the estimate $\hat{\theta}$ for the object's brightness $F = 10^4$ counts.

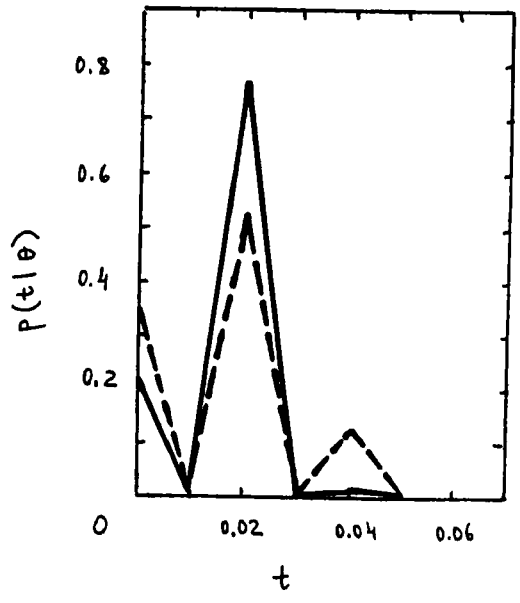

Figure 4 Sample distribution densities of $\hat{\theta}$ for $F = 10^6$ counts, true separation $\theta = 0.02$, and image pixel size $p_i = 0.01\Delta$ (solid line) and $p_i = 0.50\Delta$ (dotted line).

4 RESTORATION WITH COARSE PIXELS

In the preceding calculations, the image counts used a grid of pixels with the size of 1/100 of the PSF width Δ. Evidently, so detailed information is not necessary under exact knowledge of the PSF. According to the *sampling theorem* by La Vallee Poussin, Kotel'nikov, and Shannon (see Kolmogorov and Tikhomirov, 1959; Kotel'nikov, 1933; Shannon, 1948, 1949), it is sufficient to have sampling frequency equal to $2f_c$ in order to save completely the information about a deterministic process with maximum spectrum frequency f_c. Since, according to (3), the *Modulation Transfer Function* is

$$T(f) = \begin{cases} 1 - |f| \cdot \Delta, & \text{when } |f| \le \Delta^{-1}, \\ 0, & \text{when } |f| > \Delta^{-1}, \end{cases} \tag{9}$$

Table 2. ($F = 10^6$)

θ	p_i/Δ	$\mathfrak{N}$	$E(\hat{\theta}\|\theta) \cdot 10^2$	$var(\hat{\theta}\|\theta) \cdot 10^4$	r_p
0.02	0.01	2706	1.58±0.02	0.78±0.02	
	0.50	2706	1.56 0.03	1.70 0.05	0.36±0.02
0.10	0.01	2143	10.00 0.00	0.00	
	0.50	2143	9.998 0.001	0.004 0.0001	1.00 0.00

Table 3. $(F = 10^4, \theta = 0.10)$

p_i/Δ	$\mathfrak{N}$	r_p	$E(\hat{\theta}\|\theta) \cdot 10^2$	$var(\hat{\theta}\|\theta) \cdot 10^4$
0.01	23389	1.0	9.26±0.03	21.6±0.2
0.25	4216	0.92±0.003	8.93 0.07	23.2 0.5
0.50	4765	0.84 0.01	8.87 0.08	29.8 0.6
0.70	2129	0.65 0.01	8.93 0.13	33.6 1.0
0.80	2315	0.25 0.02	9.70 0.20	70.1 2.1
1.00	1601	0.10 0.02	0.67 0.04	2.3 0.1

we have now the critical frequency $f_c = \Delta^{-1}$, and one should put at least 2 samples at the PSF "radius" Δ to exhaust information about a non-random image. On the other hand, practically point-like samples are meant by the sampling theorem, whereas the size of image pixels is close to the separation between them. Another problem is that images have stochastic nature due both to inevitable photon noise and to random background. For these reasons, the question of detector structure for random image analysis needs special investigation. We had a good opportunity to perform some experiments with pixels of size $p_i \sim \Delta$ in the course of the simulations described above. In particular, it was interesting to clear up, how quickly the quality of restoration drops when we are crossing the "sampling border" $p_c \equiv \Delta/2$.

Figure 4 shows the sample density distributions of $\hat{\theta}$ two pixel sizes: $p_i = 0.01 \cdot \Delta$ and $p_c = 0.50 \cdot \Delta$ (the critical value). One can see that the reduction of pixel size below the critical value improves, to some extent, the reliability of restoration of bright sources, but does not change the quality in a radical way. The corresponding numerical data are given in Table 2. We denote by r_p the sample correlation coefficient between estimates of $\hat{\theta}$ for *simulations of the same image*, but for different pixel size: $0.01 \cdot \Delta$ and the current value p_i.

More extensive simulations have been performed for the case when $F = 10^4, \theta = 0.10$ (Figure 5, Table 3). One may infer again that the accuracy of restoration is somewhat better for $p_i < p_c$, whereas it is much worse for $p_i/\Delta > 0.8$.

CONCLUDING REMARKS

The results described above show that the transition from quite reliable identification of double sources to their complete indistinguishability is comparatively steep; it usually takes less than 10% of the PSF width. The accuracy of the separation estimates also decreases quickly as the components draw together. So one may hope to obtain reasonable results studying double sources in the transition region between the Rayleigh's limit and the boundary defined by Equation (1).

More extensive calculations are needed to investigate all related items in detail. Unfortunately, this is not possible for us now because of too high demands to the computer speed for Monte Carlo simulations, which are followed by restoration work.

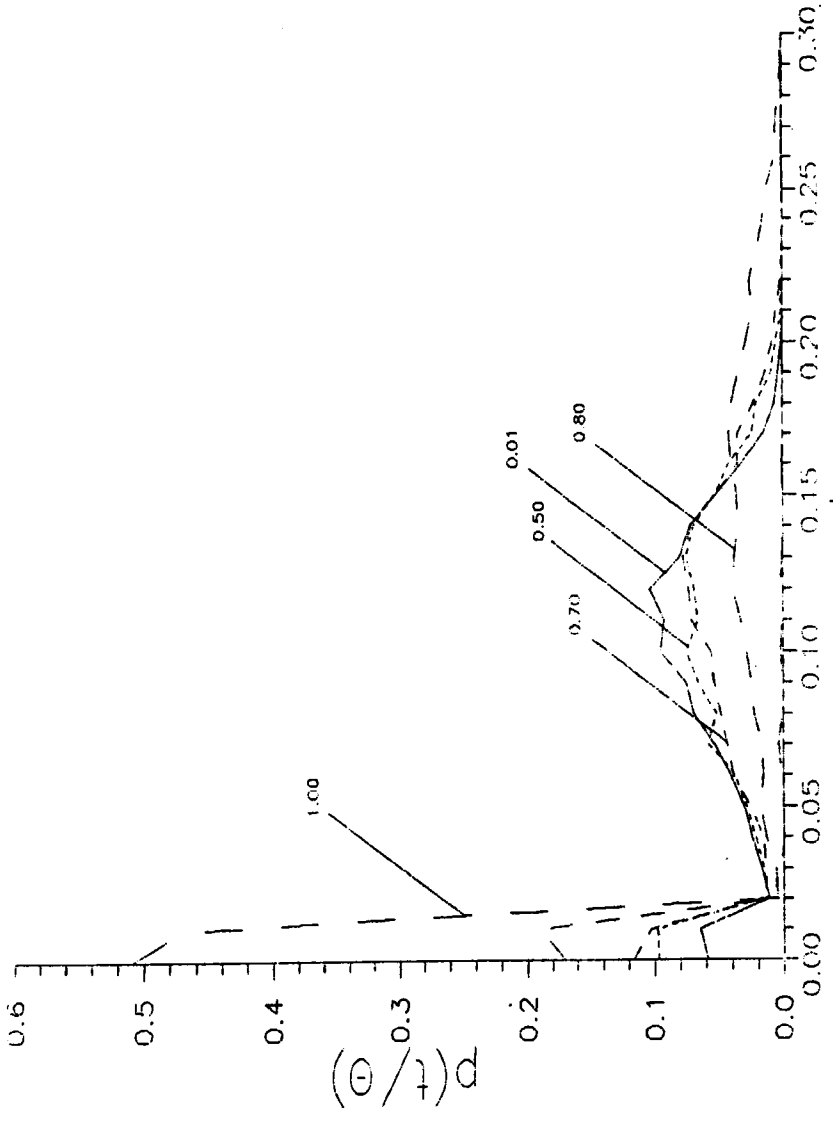

Figure 5 Sample distribution densities of $\hat{\theta}$ for various values of p_i/Δ ratio when the object's brightness is $F = 10^4$ counts and the true components' separation is $\theta = 0.10$.

The problem of accurate measurements of stellar positions is worth mentioning among many possible applications of the considered problem. Let us assume (Nesterov *et al.*, 1992) that we may acquire images of stars distant from one another with the same detector using some rigid optical system, and it is possible to consider stars as point-like objects on the basis of indirect evidence. Then using the optimal restoration procedure allows us to estimate the relative positions of stars with the theoretical accuracy, even when images are significantly overlapped and the pixel grid is coarse.

We are greatful to V. V. Biryukov and D. L. Snyder for valuable discussions.

References

Frieden, B. R. (1967) *Journ. Opt. Soc. Amer.* **57**, 1013.
Harris, J. L. (1964a) *Journ. Opt. Soc. Amer.* **54**, 606.
Harris, J. L. (1964b) *Journ. Opt. Soc. Amer.* **54**, 931.
Helstrom, C. W. (1969) *Journ. Opt. Soc. Amer.* **59**, 164.
Helstrom, C. W. (1970) *Journ. Opt. Soc. Amer.* **60**, 659.
Helstrom, C. W. (1973) *IEEE Trans. on Information Theory* **IT-19**, 389.
Kolmogorov, A. N. and Tikhomirov, V. M. (1959) *Uspekhi Matemat. Nauk* **14**, 3 (in Russian).
Kotel'nikov, V. A. (1933) *Materials to the 1-st Soviet Symp. on Technical Reconstruction of Communications and Development of Weak Current Industry*, Moscow (in Russian).
Kozlov, V. P. (1964) *Optika i Spectroscopiya* **16**, 501 (in Russian).
Llacer, J. and Veklerov, E. (1987) *IEEE Trans. on Medical Imaging* **MI- 8**, 186.
Lucy, L. B. (1992a) *Astronomical Journ.* **104**, 1260.
Lucy, L. B. (1992b) *Astronomy and Astrophysics* **261**, 706.
Nesterov, V. V., Cherepaschuk, A. M., and Sheffer, E. K. (eds.) (1992) *Space astrometric experiment "Lomonosov"*, Moscow University.
Rautian, S. G. (1958) *Uspekhi Fizich. Nauk* **66**, 475 (in Russian).
Rayleigh, Lord (J. W. Strutt) (1964) *Scientific Papers* **1**, Dover, New York.
Schelkunoff, S. A. (1943) *Bell Syst. Tech. Journ.* **22**, 80.
Shannon, C. (1948) *Bell Syst. Tech. Journ.* **27**, 379, 623.
Shannon, C. (1949) *Proc. IRE* **37**, 10.
Snyder, D. L. (1990) In *The Restoration of HST Images and Spectra*, R. L. White and R. J. Allen (eds.), Proc. of a Workshop at the Space Telescope Institute, p. 56.
Snyder, D. L. and Miller, M. I. (1985) *IEEE Trans. on Nucl. Sci.* **NS-32**, 3864.
Snyder, D. L. and Miller, M. I. (1991) *Random Point Processes in Time and Space*, Springer Verlag.
Terebizh, V. Yu. (1990) *Astrofizika* **33**, 409.
Terebizh, V. Yu. (1991) *Astronomical and Astrophysical Transactions* **1**, 3.
Terebizh, V. Yu. (1993) *Astronomy and Astrophysics* **270**, 543.
Terebizh, V. Yu. and Biryukov, V. V. (1993) *Astronomical and Astrophysical Transactions* (in press).
Toraldo di Francia, G. (1955) *Journ. Opt. Soc. Amer.* **45**, 497.
Veklerov, E. and Llacer, J. (1987) *IEEE Trans. on Medical Imaging* **MI-6**, 313.
Wolter, H. (1961) In *Progress in Optics*, E. Wolf (ed.) **1**, 155.